Radiation dose associated with coronary CT angiography and invasive coronary angiography: An experimental study of the effect of dose-saving strategies

Akmal Sabarudin MSc[1,2], Zhonghua Sun PhD[1], Kwan-Hoong Ng PhD[3]

1. Discipline of Medical Imaging, Department of Imaging and Applied Physics, Curtin University, GPO Box U1987 Perth, Western Australia, 6845.
2. Diagnostic Imaging & Radiotherapy Programme, Faculty of Allied Health Sciences, Universiti Kebangsaan Malaysia, 50300, Kuala Lumpur, Malaysia.
3. Department of Biomedical Imaging, University of Malaya, Kuala Lumpur, 50603, Malaysia.

Corresponding author:

Associate Professor Zhonghua Sun, Discipline of Medical Imaging, Department of Imaging and Applied Physics, Curtin University, GPO Box, U1987, Perth, Western Australia, 6845, Australia.

Tel: +61-8-9266 7509

Fax: +61-8-9266 2377

Email: z.sun@curtin.edu.au

Abstract

This study was conducted on a human anthropomorphic phantom to investigate the effective dose and entrance skin dose in selected radiosensitive organs through invasive and CT coronary angiography procedures using different dose-saving techniques. The effective dose was calculated as 2.49 mSv, 3.35 mSv, and 9.62 mSv respectively, corresponding to three coronary CT angiography protocols including, prospective ECG-gating, retrospective ECG-gating with and without tube current modulation. In comparison, effective dose was calculated as 7.26 mSv, 6.35 mSv, 5.58 mSv, and 4.71 mSv at four different magnifications acquired with invasive coronary angiography. The highest entrance skin dose was measured at the breast during the coronary CT angiography and at the thyroid gland during invasive coronary angiography. Although invasive coronary angiography produces lower radiation dose than coronary CT angiography, application of modified techniques in both CT and invasive coronary angiography is recommended in clinical practice for radiation dose reduction.

Keywords: Computed tomography, radiation, organ dose, dose reduction

Introduction

Invasive angiography is regarded as the gold standard technique for diagnostic and therapeutic purposes with regard to vascular diseases [1,2]. Since the emergence of the multislice CT, especially the extensive applications of CT angiography technique, invasive angiography examinations have been replaced by this less-invasive procedure with the aim of reducing procedure-related complications. Nowadays, the multislice CT angiography has become a reliable alternative to conventional angiography in many vascular applications due to its rapid technological developments, which lead to fast scanning and data acquisition with high spatial and temporal resolutions. In the United States, the numbers of CT examinations are estimated to increase gradually over the next ten years since many new applications are being developed for CT procedures to improve the diagnostic accuracy [3]. In most clinical centers, multislice CT angiography is being increasingly used to replace conventional angiography as an alternative method in vascular imaging.

One of the main applications of multislice CT angiography is coronary CT angiography, with the diagnostic value having been significantly improved with rapid technical developments from the earlier generation of the 4-slice to the latest model 320-slice CT [4,5]. Despite the high diagnostic value of coronary CT angiography, the radiation dose associated with coronary CT angiography has raised serious concerns in the medical field. In response to this concern, various dose-saving techniques have been introduced to reduce or minimize the radiation dose while acquiring diagnostic quality images. Parameters such as reduced tube voltage, prospective ECG-gating, and tube current modulations including, ECG-controlled and attenuation-dependent modulation have been reported to result in a significant dose reduction in cardiac CT [5,6]. As invasive coronary angiography is still regarded as the gold standard technique in diagnosing coronary artery disease, this procedure is retained with the

latest developments in dose-reducing strategies, for instance, spectral shaping filter, pulsed fluoroscopy in cardiac angiography, flat panel detector, continuous half exposure, and the air gap technique in order to increase the accuracy and reduce radiation dose [7,8].

During coronary CT or invasive angiography examinations, it is not unusual for some organs to receive unnecessary exposure to radiation, which leads to the dose level exceeding the acceptable limits. Many radiosensitive organs are at a potential risk of being overexposed since they are located within the radiation exposure coverage, especially the breast tissue and the thyroid gland. It has been shown that the risk of lung or breast cancer development may correlate with radiation exposure from the chest CT scan [9,10]. Therefore, those organs need to be protected and monitored as there is a direct correlation between development of thyroid cancer and radiation exposure. Although many studies suggest that protective shielding results in a significant reduction of radiation dose [11], it is not feasible to protect all of those organs as it may compromise image quality. It seems impractical to block those organs with designated shielding, which may obscure the regions of interest simultaneously. However, only certain organs are easily protected such as the thyroid gland, eyes (the lens), and the gonad but again, this depends on the type and purpose of the examination. Optimization of the technical parameters is another effective way to protect the radiosensitive organs by reducing radiation dose during CT examinations. The aim of the study was to compare the effective dose estimation (E) and entrance skin dose (ESD) of the selected radiosensitive organs through coronary CT angiography and invasive angiography performed with different protocol settings.

Material and methods

Coronary angiography equipments

This study was performed on an anthropomorphic thorax phantom to simulate an average-sized male adult with a height of 175 cm and a weight of 74 kg (Pixy, USA) with the use of a 64-slice CT scanner (Brilliance 64, Philips Healthcare, USA) and the Allura Xper FD20 with flat panel detector C-arm (Philips Medical, USA). Three coronary CT angiography protocols were set up for radiation-dose comparisons (E and ESD) including, standard retrospective gating without tube current modulation (routine protocol), retrospective ECG-gating with ECG-controlled tube current modulation (TCM), and prospective axial gating technique (dose-saving protocols). On the other hand, invasive coronary angiography procedure was performed in a series of 11 projections with four different protocols indicated by different magnifications of the flat panel detector of 1.6, 1.8, 2.2, and 2.5 magnification factors.

The ESD was measured using thermoluminescence dosemeter (TLD) rods and the E was determined by calculation from dose length product (DLP) and kerma air product (KAP). Both doses were recorded during the procedures and compared for both, CT and invasive angiography.

Coronary CT angiography protocols

Since the coronary scan is needed to be triggered by the heart rate, the electrocardiogram leads were attached to a volunteer outside the scanning room for the heart rate readings prior to the scans. No contrast medium was used in this study. Therefore, no image quality assessment was observed throughout the procedures. The coronary CT angiography was performed with a detector collimation of 64 × 0.625 mm, slice thicknesses of 0.8 mm, field of view ranging from 150 mm to 174 mm, tube voltages of 120 kV, and adjustable tube current in the range of 300–500 mA. All the scan protocols were based on the same scout image and using the same volume of coverage in order to obtain the consistency of the study pattern. Specific protocols are detailed in Table 1. The protocols were selected and modified

according to those applied in the department's routine practice. In addition, it was chosen based on previous studies which were recommended to produce a significant dose reduction as a dose-saving strategy in CT coronary angiography [5,12]. The DLP from each protocol scanned was recorded.

Invasive coronary angiography procedures

Each invasive angiography protocol consisted of 11 projections including left anterior oblique (LAO) 15°/15° caudal, LAO 30°, LAO 30°/30° caudal, LAO 40°/60° caudal, left lateral 90°, anterior-posterior (AP) 30° caudal, AP 20° cranial, AP 40° cranial, right anterior oblique (RAO) 30°/30° cranial, RAO 35°, and RAO 40°/30° caudal. In addition, the dose area product (DAP) reading from each projection was recorded once it was complete. Each projection was obtained at 100–110 cm of source-to-image distance and at approximately 80 frames of dynamic acquisition. Those projections were suggested in order to cover the entire coronary anatomy during the invasive coronary angiography procedure. The sideways collimation was applied accordingly as in clinical practice to minimize the radiation dose. The exposure filter was selected with 0.10 mmCu/1.00 mmAl and 0.9 mmCu/1.00 mmAl for fluoroscopy filtration from the angiographic system and automatic exposure control was applied. Specific protocols are recorded in Table 2.

Radiation dose measurements

ESD was measured by placing the TLD rods securely above the radiosensitive organs on the phantom skin surface. It was paramount to identify the highest point of radiation dose received by organs from the overall dose distribution which includes exposure from either the primary beam or the secondary radiation beams, depending on the location of these organs during coronary CT and invasive angiography procedures. The ESD was then recorded in milligray (mGy) after undergoing a series of procedures including annealing, calibration,

radiation dose exposure, and read-out process. The annealing and dose read-out was performed with a Harshaw-5500 reader (Thermo Electron Corp., USA) while calibration was performed with general x-ray machine (Shimadzu, Japan). TLDs calibration was designed to create a graph pattern for radiation dose conversion from nanoculomb (nC) to miligray (mGy) by exposing it to a known dose, which was measured with a digital radiation survey meter (model 660) having an ion-chamber model 660-3 beam measurement probe and a readout/logic unit (model 660-1). These TLDs were interpreted 24 hours after the exposure. The TLD used in this study was micro-rod shaped and sealed in numbered, cylindrical tubing.

A total of eighteen TLDs were securely taped on the phantom skin surface over the radiosensitive organs for each protocol whereas; three were placed on the bilateral thyroid, breast, and gonad organs in order to measure the dose distribution during the procedures. Four invasive angiography protocols were designed with different flat panel detector magnifications ranging from 19 cm to 31 cm indicating between 1.6 and 2.5 magnification factors. Similar to the coronary CT angiography procedure, 18 different TLDs were used and placed at exactly the same locations in each protocol magnification for dose comparison. The TLD readings of a specific organ were averaged to calculate the dose for this organ.

The E was obtained by straightforward calculation based on a formula. The formula required DLP from CT scans and dose area product (DAP) from invasive angiography. DAP is a quantity known to many interventionalists and it is numerically equal to the KAP which KAP is the quantity recommended by the International Commission on Radiation Units (ICRU) to measure patient doses in interventional radiology [13]. Both the DAP and the DLP were then multiplied with dose conversion co-efficient factor (DCC) distinctively. The DCC factor was derived from the parts anatomically-specific to the region of the body being scanned in CT while DCC for invasive angiography was derived from a study which met the specific exposure conditions in the coronary angiography procedure [14]. A conversion factor of 0.017

$mSv \cdot mGy^{-1} \cdot cm^{-1}$ was used for the calculation of the E in the chest region [15] in coronary CT angiography and 0.2 $mSv \cdot Gy^{-1} \cdot cm^{-2}$ was used to calculate the E in invasive coronary angiography [14,16].

Statistical analysis

All data were entered into SPSS V17.0 (SPSS, version 17.0 for Windows, Chicago, Illinois, USA) for statistical analysis. A p-value of <0.05 was considered to indicate statistically significant differences. All of the doses from each protocol were presented in box plots. One-way analysis of variance (ANOVA) and repeated measures ANOVA were used in ESDs analysis to determine the existing difference in mean ESD of radiosensitive organs (thyroid, breast and gonad) in both CT and invasive coronary angiography of all protocols. With regard to the effective dose, the ANOVA test was performed to determine the significant difference of mean values between the protocols. Moreover, a Duncan multiple range test was used to facilitate statistical comparisons among the mean values in invasive coronary projections.

Results

Coronary CT angiography

There were no significant differences in ESD measurements between the radiosensitive organs as tested with one-way ANOVA ($p=0.32$). However, with use of repeated measures ANOVA, the ESD measured in thyroid, breast and gonad differed significantly within all three protocols (standard retrospective ECG gating, retrospective ECG gating with tube current modulation and prospective ECG gating) ($p<0.05$). ESD was found to be the highest at the breast compared to other organs with a mean value of 79.2 ± 1.1 mGy acquired with standard retrospective gating (protocol 1), 34.7 ± 1.9 mGy with prospective ECG-gating

technique (protocol 2), and 38.6 ± 0.1 mGy with retrospective with tube current modulation (protocol 3) (Figure 1). The dose received by the breast was six times greater than that by the thyroid during the procedure.

The DLP was recorded individually for dose comparison among the three protocols with the inclusion of effective dose estimation. Statistically significant differences were found between the mean E values among different protocols ($p<0.001$). The mean E demonstrated that the standard retrospective gating protocol (protocol 1) resulted in the highest dose of 9.6 ± 0.1 mSv, followed by retrospective gating with tube current modulation (protocol 3) (3.3 ± 0.5 mSv), and prospective gating (protocol 2) (2.5 ± 0.8 mSv).

Invasive coronary angiography

Entrance skin dose was measured and recorded for all three radiosensitive organs (the thyroid, the gonads, and the breast) in all four protocols (1.6, 1.8, 2.2, and 2.5 magnification factor). Overall, there was no significant difference in ESD between radiosensitive organs (thyroid, breast and gonad) as tested with one-way ANOVA at $p=0.26$. However, on further examination with the repeated measures ANOVA, there was significant difference in ESD within the protocols. In other words, the changes in dose received by organ is significant when the magnification increased or decreased with $p<0.05$. Therefore, thyroid gland returns with higher scores than breast and gonad in all protocols with resultant 3.2 ± 0.7 mGy, 2.0 ± 0.4 mGy, 1.6 ± 0.2 mGy, and 1.4 ± 0.3 mGy corresponding to 1.6 (protocol 1), 1.8 (protocol 2), 2.2 (protocol 3), and 2.5 flat panel detector magnifications (protocol 4). .

Different magnifications of flat panel detector indicated dose variations among all 11 projections during invasive coronary angiography. The DAP was recorded to determine the radiation dose production in each projection (Table 3). The results showed that the LAO 60° with caudal 40° (spider view) projection produced the highest dose which is about 2.3 times

higher than the average dose of overall projections, which is statistically significant as tested with Duncan's multiple comparisons. The effective dose estimation was calculated then from the DAP of total projections at the end of each examination to compare the protocols. The mean E differed significantly across all magnification settings with ANOVA test at $p < 0.05$. Results showed the highest mean E estimation was 7.2 ± 0.05 mSv calculated at 1.6 FD magnifications (protocol 1). The effective dose was reduced significantly with 6.4 ± 0.05 mSv, 5.6 ± 0.01mSv, and 4.7 ± 0.07 mSv ($p<0.05$) being achieved and corresponding to the smaller magnifications of 1.8 (protocol 2), 2.2 (protocol 3), and 2.5 (protocol 4), respectively.

Discussion

This study demonstrates four important findings of radiation dose reduction in coronary angiography using CT angiography and the invasive approach. Firstly, coronary CT angiography results in an effective dose that is about 2.5 times higher than that of invasive angiography. Secondly, dose-saving protocols in coronary CT angiography (prospective gating and attenuation dependent tube current modulation) help to reduce the effective dose significantly up to 70% when compared with a standard retrospective gating. Thirdly, effective dose arising from invasive angiography is decreased up to 13% with an increase in magnifications. Finally, invasive angiography leads to a significant reduction in entrance skin dose up to 95% compared to CT coronary angiography at three radiosensitive organs (the thyroid, the breast, and the gonads).

Many studies have reported that the prospective ECG-gating reduces effective dose significantly between 60% and 90% when compared with retrospective ECG-gating [17,18]. The prospective gating uses a step-and-shoot technique with the radiation beam turned on only at selected cardiac phase, and turned off for the remaining cardiac cycle to keep the dose

to a minimum. This is confirmed in our results as the prospective ECG-gating reduces the effective dose by up to 70% compared with retrospective gating.

Radiation dose in CT can be reduced significantly by applying the approach of tube current modulation. Either ECG-controlled or anatomical-dependent tube current modulation results in effective dose reduction significantly between 22% and 52% compared to retrospective ECG-gating without any modifications [19,20]. In ECG-controlled modulation, the tube current is reduced to the level between 46% and 80% from its maximum at diastole (60–80% of R-R interval) [19]. Our findings are consistent with these reports as the results demonstrate a significant reduction of about 65% in effective dose with ECG-controlled tube current modulation when compared with the corresponding retrospective gating.

The entrance skin dose received by each organ varies differently in coronary CT and invasive coronary angiography. This is because of the distance between the x-ray tube and the response organ during the exposure and their locations. For example, in CT coronary angiography, the cardiac phantom was positioned at the center of the x-ray tube so that the breast would receive the maximum dose from the primary radiation beam. However, the thyroid and the gonad only received scattered radiation since they were anatomically situated away from the breast. This was verified by the TLD measurement in our study. In invasive angiography, the situation was slightly different. The measured thyroid gland dose was the highest compared to that from the breast and the gonad. The caudal tube angulation brings the x-ray tube closer to the thyroid gland and results in increased radiation dose as stated in the inverse square law.[21] Moreover, the repetition of caudal tube angulation performed in this study (6 out of 11) explained the fact that the thyroid gland received higher radiation dose than other organs.

Although radiation dose values in both, CT and invasive angiography, such as DAP, air kerma, DLP, and the CT dose index could not be compared directly due to different

measurement units, the estimations of effective dose is still measureable and comparable in those angiographic systems. Effective dose represents a general dose quantification of the biological risk in medical exposure where it is not a quantity that can be measured independently. It can only be derived by computation from a model or simulation that has estimated the dose for individual tissues [22]. Our study estimates the effective dose in all protocols of CT and invasive angiography for comparison. It is essential to provide information and create awareness about radiation dose in angiography among patients, Radiologists, imaging technologists, and the public.

Our study investigates 11 common projections in invasive coronary angiography to cover all the cardiac vessels. The left anterior oblique/caudal (spider view) is shown with 3 times higher dose production compared to other projections. This was reported as being similar to a previous study by Kuon et al,[21] where the dose was increased up to 2.6 times and 3.7 times higher when the angulation was continuously raised from right to left anterior oblique and cranial to caudal tube angulation, respectively. However, the dose was reported to be decreased significantly with every 10° decrement in tube angulations. Since this view is important to optimize the visualization of the left circumflex artery with obtuse marginal, left main artery, bifurcation of left anterior descending and the diagonal artery, therefore, there is no other option but to reduce the dose by eliminating this projection other than limiting the angulation and regulating the time duration of the exposure wisely.

The entrance skin dose was taken into consideration in this study since it predicted the possibility of getting deterministic skin injuries ranging from skin erythema, moist desquamation, epilation, laceration, to necrosis if the skin was exposed beyond the threshold dose at 2 Gy [23]. Deterministic injuries to the skin are associated with overexposure regardless of high radiation exposure setting or increased length of exposure. Therefore, 45 $Gy \cdot cm^2$ was proposed as the diagnostic reference level for coronary angiography by the

European Commission DUMOND III project in 2003 in order to prevent the interventionalist from going beyond that dose threshold [24]. However, even though the skin received a radiation dose below the dose threshold, it was still at the risk of developing radiation-induced cancer from the stochastic effects.

Our study has its limitations. Although the protocols were developed from previous reports in the literature on CT dose-saving strategies, it is still difficult to measure the accuracy on the protocol guideline since the image quality assessment has not been taken into account. However, this study only used an anthropomorphic phantom to simulate the radiation dose quantification on a standardized patient. No contrast medium was used in any of the angiography protocols. Therefore, there is no way of comparing and assessing image quality, since no contrast enhancement in the coronary arteries could be visualized. Thus, further studies are necessary to verify the accuracy of our results through the administration of a contrast medium and qualitative and quantitative assessment of image quality.

In conclusion, this study shows that invasive angiography produces significantly lower radiation dose than coronary CT angiography, which is demonstrated by effective dose and entrance skin dose. Modification techniques in coronary CT (dose-saving protocols) and invasive angiography (multi-size magnification) are recommended in daily clinical practice since they produce further dose reduction.

References

1. Tan, K., Reed, D., Howe, J., Challenor, V., Gibson, M. and McGann, G. *CT vs conventional angiography in unselected patients with suspected coronary heart disease.* Int J Cardiol **121**, 125–126 (2007).
2. Tins, B., Oxtoby, J. and Patel, S. *Comparison of CT angiography in aortoilliac occlusive disease.* Br J Radiol **74,** 219–225 (2001).
3. National Council on Radiation Protection and Measurements. *Ionizing radiation exposure of the population of the United States, in Computed Tomography.* National Council on Radiation Protection and Measurements, Bethesda. 85–96 (2009).
4. Hein, P. A., Romano, V. C., Lembcke, A., May J. and Rogalla, P. *Initial experience with a chest pain protocol using 320-slice volume MDCT.* Eur Radiol **19**, 1148–1155 (2009).
5. Sun, Z., Choo, G. H. , Ng, K. H. *Coronary CT angiography: current status and continuing challenges.* Br J Radiol (in press).
6. Sun, Z. and Ng, K. H. *Multislice CT angiography in cardiac imaging-part III: radiation risk and dose reduction.* Singapore Med J **51**, 374–380 (2010).
7. Lederman, H. M., Khademian, Z. P., Felice, M. and Hurh, P. J. *Dose reduction fluoroscopy in pediatrics.* Pediatr Radiol **32**, 844–848 (2002).
8. Partridge, J., McGahan, G., Causton, S., Bowers, M., Mason, M., Dalby, M. and Mitchell, A. *Radiation dose reduction without compromise of image quality in cardiac angiography and intervention with the use of a flat panel detector without an antiscatter grid.* Heart **92**, 507–510 (2006).
9. Preston DL, Ron E, Tokuoka S, Funamoto S, Nishi N, Soda M, Mabuchi K, Kodama K. *Solid cancer incidence in atomic bomb survivors: 1958–1998*. Radiat Res **168**, 1–64 (2007)

10. Angel, E., Yaghmai, N., Jude, C. M., DeMarco, J. J., Cagnon, C. H., Goldin, J. G., McCollough, C. H., Primak, A. N., Cody, D. D., Stevens, D. M. et al. *Dose to radiosensitive organs during routine chest CT: effects of tube current modulation.* Am J Roentgenol **193**, 1340–1345 (2009).

11. McLaughlin, D. J. and Mooney, R. B. *Dose reduction to radiosensitive tissues in CT. Do commercially available shields meet the users' needs?* Clin Radiol **59**, 446–450 (2004).

12. Kalra, M. K., Maher, M. M., Toth, T. L., Schmidt, B., Westerman, B. L., Morgan, H. T. and Saini, S. *Techniques and applications of automatic tube current modulation for CT.* Radiology **233**, 649–657 (2004).

13. Vano, E., Sanchez, R., Fernandez, J. M., Gallego, J. J., Verdu, J. F., Gonzalez de Garay, M., Azpiazu, A., Segarra, A., Hernandez, M. T., Canis, M., Diaz, F., Moreno, F., Palmero, J. *Patient dose reference levels for interventional radiology: a national approach.* Cardiovasc Intervent Radiol **32**, 19–24 (2009).

14. Schultz, F. W. and Zoetelief, J. *Dose conversion coefficients for interventional procedures.* Radiat Prot Dosim **117**, 225–230 (2005).

15. Huda, W., Ogden, K. M. and Khorasani, M. R. *Converting dose-length product to effective dose at CT.* Radiology **248**, 995–1003 (2008).

16. Broadhead, D. A., Chapple, C. L., Faulkner, K., Davies, M. L. and McCallum, H. *The impact of cardiology on the collective effective dose in the North of England.* Br J Radiol **70**, 492–497 (1997).

17. Earls, J. P. *How to use a prospective gated technique for cardiac CT.* J Cardiovasc Comput Tomogr **3**, 45–51 (2009).

18. Freeman, A. P., Comerford, R., Lambros, J., Eggleton, S. and Friedman, D. *64 slice CT coronary angiography-marked reduction in radiation dose using prospective gating.* Heart, Lung Circ **18**, S13–S13 (2009).

19. Mayo, J. R., and Leipsic, J. A. *Radiation dose in cardiac CT*. Am J Roentgenol **192**, 646–653 (2009).

20. Greess, H., Lutze, J., Nömayr, A., Wolf, H., Hothorn, T., Kalender, W. A. and Bautz, W. *Dose reduction in subsecond multislice spiral CT examination of children by online tube current modulation.* Eur Radiol **14**, 995–999 (2004).

21. Kuon, E., Dahm, J. B., Empen, K., Robinson, D. M., Reuter, G. and Wucherer, M. *Identification of less-irradiating tube angulations in invasive cardiology*. J Am Coll Cardiol **4**, 1420–1428 (2004).

22. Martin, C. J. *Effective dose: how should it be applied to medical exposures?* Br J Radiol **80,** 639–647 (2007).

23. Bogaert, E., Bacher, K., Lemmens, K., Carlier, M., Desmet, W., Wagter, X. D., Djian, D., Hanet, C., Heyndrickx, G., Legrand, V., Taeymans, Y., Thierens, H. *A large-scale multicentre study of patient skin doses in interventional cardiology: dose-area product action levels and dose reference levels.* Br J Radiol **82**, 303–312 (2009).

24. Neofotistou, V., Vano, E., Padovani, R., Kotre, J., Dowling, A., Toivonen, M., Kottou, S., Tsapaki, V., Willis, S., Bernardi, G., Faulkner, K. *Preliminary reference levels in interventional cardiology*. Eur Radiol **13**, 2259–2263(2003).

Figure legends

Figure 1. Box plot shows the mean ESD of 3 radiosensitive organs (the thyroid, breast, and gonad) in CT coronary angiography. It shows that the breast received the highest dose distribution compared to the thyroid and gonad in prospective gating, retrospective gating with and without tube current modulation. The boxes indicate the first to third quartiles, and each midline indicates the median (second quartile) and the whiskers represent the maximum and minimum values of ESD.

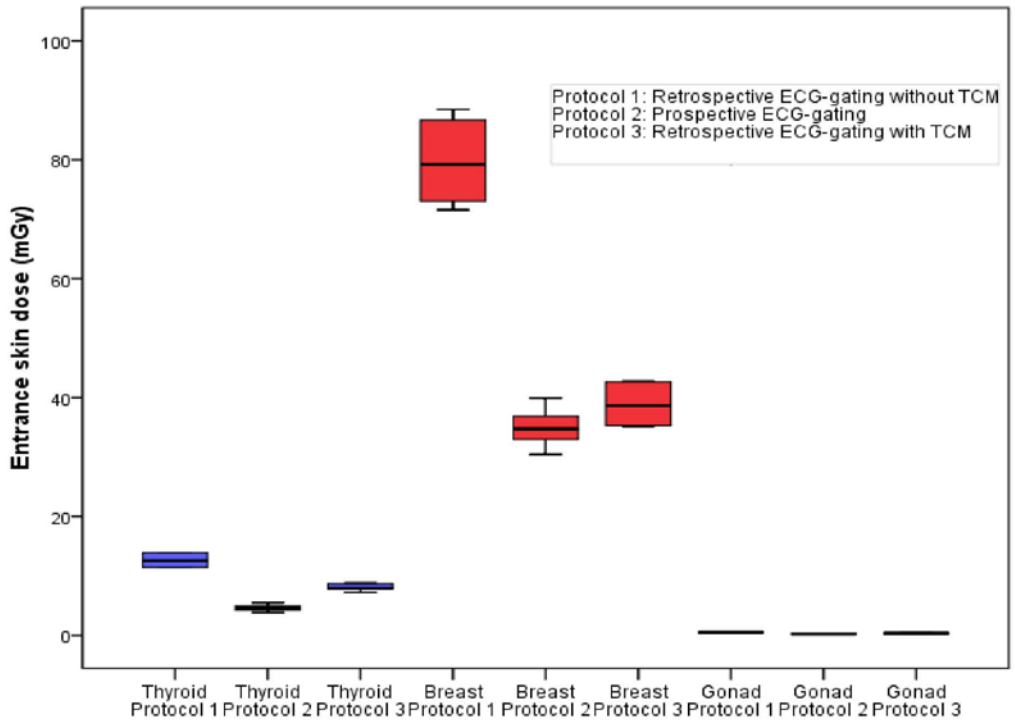

Figure 2. Distribution of mean ESD measured at 3 radiosensitive organs (the thyroid, breast, and gonad) in invasive coronary angiography with the use of different magnification factors displayed by the box plot. Apparently, the thyroid gland received the highest radiation dose compared to breast and gonad in all 4 protocols. However, it still remains below 3 mGy

which meets the reference dose limit set by European Commission DUMOND III project (2003). The boxes indicate the first to third quartiles, and each midline indicates the median (second quartile) and the whiskers represent the maximum and minimum values of ESD.